PREDICTING WATER QUALITY BY RELATING SECCHI DISK TRANSPARENCY DEPTHS TO LANDSAT 8

Miranda J. Hancock

Submitted to the faculty of the University Graduate School

in partial fulfillment of the requirements

for the degree

Master of Science

in the Department of Geography,

Indiana University

August 2015

Accepted by the Graduate Faculty, Indiana University, in partial

fulfillment of the requirements for the degree of Master of Science.

Master's Thesis Committee

Vijay O. Lulla, Ph.D , Chair

Daniel P. Johnson, Ph.D.

Frederick L. Bein, Ph.D.

ACKNOWLEDGEMENTS

I would like to thank the professors and staff of the Geography department; their knowledge and guidance has made this process a positive, enjoyable experience. I would like to specifically thank my Graduate Advisor, Vijay Lulla. Vijay's expertise, enthusiasm, and guidance helped to make the completion of this thesis possible.

I would like to thank my good friend, Chris Duvall, for offering up his boat to use for data collection at Brookville Reservoir. This project would not have gone as smoothly without his kindness. I would like to thank my sister, Hannah, for the numerous peer reviews she has provided over the last few years. She was always available to help, despite her busy schedule, and it has been greatly appreciated.

A final, special thank you goes to my husband Marc. His support, encouragement, and patience have been instrumental to my success. I am incredibly excited to be completing this project, and I cannot adequately express how grateful I am to Marc for his advice and support.

Miranda J. Hancock

PREDICTING WATER QUALITY BY RELATING SECCHI DISK TRANSPARENCY DEPTHS TO LANDSAT 8

Monitoring lake quality remotely offers an economically feasible approach as opposed to in-situ field data collection. Researchers have demonstrated that lake clarity can be successfully monitored through the analysis of remote sensing. Evaluating satellite imagery, as a means of water quality detection, offers a practical way to assess lake clarity across large areas, enabling researchers to conduct comparisons on a large spatial scale. Landsat data offers free access to frequent and recurring satellite images. This allows researchers the ability to make temporal comparisons regarding lake water quality. Lake water quality is related to turbidity which is associated with clarity. Lake clarity is a strong indicator of lake health and overall water quality. The possibility of detecting and monitoring lake clarity using Landsat8 mean brightness values is discussed in this report. Lake clarity is analyzed in three different reservoirs for this study; Brookeville, Geist, and Eagle Creek. In-situ measurements obtained from Brookeville Reservoir were used to calibrate reflectance from Landsat 8's Operational Land Imager (OLI) satellite. Results indicated a correlation between turbidity and brightness values, which are highly correlated in algal dominated lakes.

Vijay O Lulla, Ph.D., Chair

TABLE OF CONTENTS

LIST OF TABLES

LIST OF FIGURES

Introduction

As lake clarity and turbidity are one in the same for the scope of this study, it is important to understand turbidity. Turbidity measures the degree at which water loses its transparency due to the presence of suspended particulates. The higher the level of suspended particulates, including algae, the murkier the water.

Algae are commonly found in Indiana lakes and streams. A moderate concentration of algae is necessary for biologically productive, healthy lakes. However, excessive concentrations of algae can be linked to some adverse health effects and higher levels of waterbody turbidity. Excessive concentrations of algae negatively impact the ecological balance of lakes in the form of diminished recreations use, fish kill, and possible contamination of drinking water supplies. The water bodies examined in this paper, Brookeville Reservoir, Eagle Creek Reservoir, and Geist Reservoir have experienced regular seasonal algal blooms (Indiana Department of Environmental Management , 2015).

Factors promoting algal blooms stem from a combination of physical and chemical factors including available nutrients, temperature, sunlight, turbidity, hydrology, pH and salinity. The exact combination of factors that cause and support an algal bloom is not well understood and it is not possible to contribute blooms to a specific factor or combination of factors (Center for Earth and Environmental Science, 2015; Schlacher, Lloyd, & Wiegand, 2010). Eagle Creek and Geist reservoirs are on the Federal Clean Water Act list of impaired water bodies. Water bodies are placed on this list when they are considered too polluted or otherwise degraded and unable to meet water quality standards set by their governing authorities. The two reservoirs are on this list due, in part, to high Chlorophyll-a (algae) concentrations. (Table 1). Brookville reservoir is on the impaired water bodies list due to polychlorinated biphenyls (PCBs) in fish tissue. PCBs are not directly related to algal blooms, however Brookville reservoir has algae bloom issues and the reservoir is being closely watched by state and federal environmental agencies.

Impaired Waters Results

Description of this table

NOTE: Click on the underlined "Waterbody Name" to view the waterbody report.

Waterbody Name	Waterbody ID	Most Current Data Available	Location	Map	Waterbody Type	Size	Unit	Status	State TMDL Development Status
Geist Reservoir	INW01P1048_00	2008	Not Reported	Waterbody Map	Lakes, Reservoirs, and Ponds		Acres	Impaired	TMDL needed
Eagle Creek Reservoir	INW01P1069_00	2008	Not Reported	Waterbody Map	Lakes, Reservoirs, and Ponds		Acres	Impaired	TMDL needed
Fishback Creek (Eagle Creek Reservoir)	INW01C9_00	2008	Marion Co	Waterbody Map	Rivers and Streams		Miles	Impaired	TMDL needed
Brookville Reservoir	ING03P1019_00	2008	Not Reported	Waterbody Map	Lakes, Reservoirs, and Ponds		Acres	Impaired	TMDL needed

Table 1: EPA Status of Brookville, Geist, and Eagle Creek Reservoirs in Central Indiana

Retrieved from http://ofmpub.epa.gov/waters10/attains_index.control

Globally, algae blooms are an increasing problem in all types of waterbodies due to rising water temperatures, increases in atmospheric carbon dioxide concentrations, and changes in rainfall patterns, to name a few (United States Environmental Protection Agency, 2013). Nutrients, as mentioned above, are recognized as one of the most notorious promoters and supporters of algae growth. Nutrients, in the form of phosphorus and nitrogen, permeate through waterbodies internally and externally. External nutrient sources come from runoff and soil erosion of fertilized lawns and fields, deforested areas and sewage effluent. Internal nutrient sources consist of phosphates that attach to sediments in the waterbody.

Nutrient rich water contains low levels of oxygen availability and as such promote sediments to release those attached phosphates into the water thus encouraging the growth of algae. Without productivity and dissolved oxygen, the waterbody is unable to support beneficial and necessary organisms (Center for Earth and Environmental Science, 2015). Measuring lake clarity is an important part of evaluating algae levels and lake water quality. For example, Lake

Erie has shown signs of yearly blooms during summer months since 2008 according to the National Center for Coastal Ocean Science. (Wynne, 2013)

Because of legislation and citizen concern, a water sampling program has been undertaken by the Indiana Department of Environmental Management (IDEM), the Indiana Department of Natural Resources (DNR), the Indiana State Department of Health (ISDH), and the Board of Animal Health (BOAH). Each year, these organizations work to study, monitor, and sample algal blooms in Indiana lakes. For the 2014 sampling season, IDEM sampled for blue-green algae and processed those samples according to type and quantity of blue-green algae, as well as for microcystin, sylindrospermopsin, and anatoxin-a, toxins associated with blue-green algae.

Indiana uses the World Health Organization (WHO) guideline level of 100,000 cells/ml or microcystin toxin level of 6 parts per billion (ppb) to indicate a high cell count advisory. Beaches in Indiana close if the microcystin toxin level reaches 20ppb for a waterbody. Indiana uses the guideline of 5ppb of cylindrospermopsin and 80 ppb of anatoxin-a for a high cell count advisory. Citizens are notified via various media outlets if toxins reach threshold levels. This compilation of state-collected water quality data provides an opportunity to evaluate Indiana lakes and keep lake users safe and informed. For the 2014 sampling year, the IDEM reported a high cell count for Brookville Reservoir on August 19, 2014. High cell counts were also reported for Geist and Eagle Creek Reservoirs on August 26, 2014 (Indiana Department of Environmental Management , 2015).

This study of water quality data focuses on using remotely sensed satellite data to monitor inland lake quality. Satellites have been shown to provide a greater amount of spatial information at an improved cost compared to spot sampling programs like those administered by state organizations described above. Satellite-based measurements may provide a mechanism for early detection of blooms and/or the detection of hot-spots in unsampled or unreachable locations (Kloiber, Brezonik, Olmanson, & Bauer, 2002).

Background

Remote Sensing and Water Quality

Landsat imagery has been used for remote sensing of water quality (Brezonik,Menken, & Bauer, 2005; Fuller & Minnerick, 2001-2006). Previous studies have also shown that water clarity and Landsat data have an established relationship (Kloiber, Brezonik, Olmanson, & Bauer, 2002; Tebbs, Remediios, & Harper, 2013; Bonansea, Rodriguez, Pinotti, & Ferrero, 2014). Kloiber et al. (2002) identify similar results between secchi disk transparency (SDT) depth and Landsat data due to the underlying physical basis and the spectroradiometer's ability to collect hyperspectral reflectance data. Likewise, researchers have acknowledged that spectral features of lakes are consistently related to optically active substances including suspended sediment which contributes to turbidity (Jensen J. R., 1983). The spectral features that are of upmost interest to this study stem from sources that make-up total radiance (L_t). Total Radiance is recorded by Landsat 8 as a function of electromagnetic energy of four sources, whereas $L_t = L_p + L_s + L_v + L_b$ (Jensen J. R., 2007). L_v deals with a portion of radiance from the downwelling of solar and sky radiation that penetrates the air-water interface and interacts with the water and organic/inorganic constituents, like algae, and then exits the water column without encountering the waterbody floor (Jensen J. R., 2007). The radiance information captured here can then be transformed to brightness temperatures or values and, as a result, provide valuable information about the organic/inorganic matter contained within the waterbody. When the main goal of a study is to identify or provide information about organic/inorganic matter in the water column, it is important to avoid the L_b source of radiation. L_b is the portion of radiation that infiltrates the air-water network and reaches the bottom of the water body and then moves back up through the water body to then exit the water column. Radiance from this source (L_b) or from the bottom of a water body makes characterizing the water column above the bottom difficult (Jensen J. R., 2007). Due to the L_b source of radiation Olmansen et al. (2002) recommend collecting samples in water that is 15 feet or deeper.

Estimating turbidity via Landsat data has limitations that must be taken into consideration. Remote sensing of lakes has been known to be problematic as lakes are different in terms of the surrounding land use, ecology and water chemistry (Olmanson, Kloiber, Bauer, & Brezonik, 2001; Tebbs, Remedios, & Harper, 2013). Studies have identified a number of satellite sensors like MODIS, MERIS, SeaWiFS, MASTER and more that have been used to quantitatively monitor lake water quality (Tebbs, Remediios, & Harper, 2013; Kudela, et al., 2015). In this study, a high spatial resolution is necessary as the study area lakes are small (about 2 km across). Due to the small lake size Landsat 8's Operational Land Imager (OLI) was chosen because it posseses a high spatial resolution of 30 meters in the visible, near-infrared, and short-wave infrared bands. The high resolution allows for better detection of small scale spatial variability across the lakes of interest. Similarly, the OLI predeccessor (ETM+) was chosen for these same reasons as in the study by Tebbs et al.,2013.

The satellite sensor, in this case Landsat 8, must be able to relate a characteristic of the waterbody to an "inherent optical property" in order to extract brightness values (Brezonik, Menken, & Bauer, 2005). In this study, the characteristic is SDT and the "inherent optical property" is the radiance measured by Landsat 8 within the spectral bands of interest. Estimation limitations or errors may arise from atmospheric conditions through incoming solar radiation penetrating the water surface and then leaving the water column then reaching the satellite sensor. The intensity of solar radiations varies by latitude, season, time of day, and weather conditions. Because atmospheric conditions, sensor response, and incoming irradiance change with time it is not recommended to compare asynchronous Landsat data with in situ measurements (Brezonik, Menken, & Bauer, 2005).

Landsat

The Landsat Missions began in 1972 with Landsat 1 and have continued through to the current operation of Landsat 8 (Figure 2).

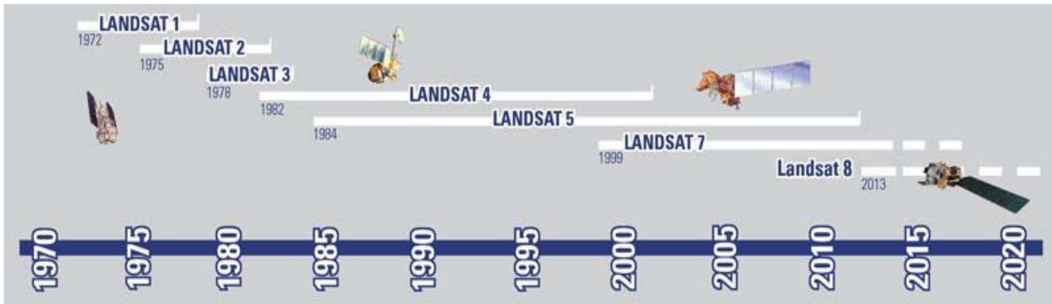

Figure 1: Timeline of Landsat Missions

Retrieved from http://www.USGS.gov

On February 11, 2013, Landsat 8 launched from Vandenberg Air Force Base, California. The Landsat 8 satellite is different from previous Landsat missions as it carries two push-broom instruments, the Operational Land Imager (OLI) and the Thermal Infrared Sensor (TIRS). The OLI sensor is similar to Landsat 7's Enhanced Thematic Mapper Plus (ETM+) except that the OLI sensor has two additional spectral bands (U.S. Geological Survery, 2015) . As this study works to apply satellite imagery to regional assessment of lake clarity using Operational Land Imager (OLI) bands found within Landsat 8, it also works to create a better understanding of Landsat 8's capabilities through water quality monitoring using OLI's spectrally narrower bands. Landsat 8 bands 3 and 4 have been used with success in this study. Band 4 (red) has been improved to a narrower wavelength (0.64 - 0.67) and is designed for improved sensitivity to discriminate vegetation slopes. Previously in Landsat 7, the red band had a wider wavelength (0.63 - 0.69) and was not as sensitive to vegetation slopes. Slope-based vegetation indices are a combination of visible red and near infrared. This combination indicates a state of abundance of vegetation cover and biomass (Roy, et al., 2014). Band 3 (green) has been improved to a wavelength of

0.53-0.59. This band is useful in assessing plant vigor. Plant vigor is expressed through algal blooms via phosphorus or nitrogen loading.

As Sriwongsitanon, Surakit, & Thianpopirug (2011) explain, there is no standard prediction equation for water quality parameters for images collected on different dates for the same location. Conversely, prediction models are getting close on a standardized model for images contemporaneously taken with field samples. This study will utilize Landsat 8 band 3 and band 4 to further validate the possibility that water quality monitoring through satellite imagery can be a standardized process.

OLI has a deep blue visible channel (band 2) that is designed specifically for water resources and coastal zone analysis as well as an infrared channel (band 9) that can be utilized for the detection of cirrus clouds. The TIRS sensor collects two spectral bands (bands 10 and 11) for the wavelength previously covered by one band (band 6) on Landsat 7. The Landsat 8 sensors provide seasonal coverage at a spatial resolution of 30 meters (visible, NIR, SWIR); 100 meters (thermal); and 15 meters (panchromatic). (Landsat Science, 2014) Landsat 8 provides significant improvement in data quality and radiometric quantization than in previous Landsat sensors. Landsat 8 radiometric quantization is 12-bits whereas the Thematic Mapper (TM) and ETM+ is 8-bits. Landsat 8 data is collected and archived every 16 days. However, cloud cover on acquisition dates may result in a lower frequency of useable data.

Landsat 8 has eight OLI, 30 meter spatial resolution, multispectral bands (Figure 4): (1) Coastal; 0.43 - 0.45 µm; (2) Blue 0.45 - 0.51 µm; (3) Green 0.53 - 0.59 µm; (4) Red0.64 - 0.67 µm; (5) NIR 0.85 - 0.88 µm; (6) SWIR1 1.57 – 1.65 µm; (7) SWIR2 2.11 – 2.29 µm; and, (9) Cirrus 1.36 – 1.38 µm. Landsat 8 also has one OLI panchromatic band, 15 meter spatial resolution: (8) 0.50 - 0.68 µm and two, 100 meter spatial resolution TIRS bands: (10) TIRS1 10.6 – 11.19 µm and (11)

TIRS2 11.5-12.51 µm. The two TIRS bands are resampled to 30 meters to match the OLI multispectral bands. Landsat 8 data is delivered as ".tar.gz" compressed files via HTTP Download. Each file is approximately 1GB (compressed) and 2GB (uncompressed). As this study utilizes landsat 8 bands (3) 0.53 – 0.59 µm and (4) 0.64 – 0.67 µm other studies have also found success when using these ranges to estimate turbidity. (Brezonik, Menken, & Bauer, Landsat-based Remote Sensing of Lake Water Quality Characteristics, Including Chlorophyll and Colored Dissolved Organic Matter (CDOM), 2005). Landsat 8 bands 5-11 provide measures of radiance in the mid-and thermal-infrared regions and have not shown use when trying to estimate water characteristics like SDT, chlorophyll, or turbidity (Brezonik, Menken, & Bauer, Landsat-based Remote Sensing of Lake Water Quality Characteristics, Including Chlorophyll and Colored Dissolved Organic Matter (CDOM), 2005).

Table 2: Landsat 8 Band Designations

Landsat 8 Operational Land Imager (OLI) and Thermal Infrared Sensor (TIRS) **Launched February 11, 2013**	**Bands**	**Wavelength (micrometers)**	**Resolution (meters)**
	Band 1 - Coastal aerosol	0.43 - 0.45	30
	Band 2 - Blue	0.45 - 0.51	30
	Band 3 - Green	0.53 - 0.59	30
	Band 4 - Red	0.64 - 0.67	30
	Band 5 - Near Infrared (NIR)	0.85 - 0.88	30
	Band 6 - SWIR 1	1.57 - 1.65	30
	Band 7 - SWIR 2	2.11 - 2.29	30
	Band 8 - Panchromatic	0.50 - 0.68	15
	Band 9 - Cirrus	1.36 - 1.38	30
	Band 10 - Thermal Infrared (TIRS) 1	10.60 - 11.19	100 * (30)
	Band 11 - Thermal Infrared (TIRS) 2	11.50 - 12.51	100 * (30)

Retrieved from http://www.USGS.gov

For this study, OLI spectral bands have been chosen because they are narrower than the ETM+ (Landsat 7) bands and have the ability to avoid atmospheric absorption features. As mentioned above, the 15 meter and 30 meter resolution of the OLI sensors gives researchers a chance, for the first time, to access the world's lakes at a high spatial resolution and positional accuracy. The OLI bands have been designed to incorporate technical advancements that improve performance over the previous Landsat sensors (Roy, et al., 2014). One significant change from Landsat 7 to Landsat 8 is that the OLI sensors are pushbroom with focal planes aligning long arrays of detectors across-track. Previous Landsat instruments used whisk-broom sensors.

Some of the benefits to using pushbroom sensors include less pixel distortion, longer dwelling time, narrow swath width, simple mechanical system, and a complex optical system. The whiskbroom sensors operate with pixel distortion, shorter dwelling time, and wider swath width to name a few. Pushbroom sensors offer improved geometric fidelity, radiometric resolution, and signal-to-noise characteristics compared to the whiskbroom sensors.

In addition to the upgraded pushbroom sensors, Landsat 8 OLI bands operate with a high or very specific signal-to-noise ratio (SNR). A high SNR is an important factor for water constituent mapping because of the very low signal that water generates. The low signal creates the variations in water quality to be lost in the noise of lower or less specific SNR systems. Previous Landsat instruments have limited capability to map water quality due to the low SNR as well as a limited number of spectral bands in the visible region where water quality spectral signatures manifest. As a result of the improved SNR, the new OLI blue band should reduce error in water constituent retrieval values by half of the error expected from Landsat 7. Landsat 8 has the potential to bring about a new era of water quality monitoring. (Roy et al., 2014)

Secchi Disk Transparency and Landsat

Water cleanliness is directly related to its turbidity (Bruckner,2013.) Waters with low turbidity contain low levels of total suspended solids (TSS) and are considered clearer than waters with high levels of TSS. Waters with a high level of turbidity block light from reaching deep into the water column creating adverse conditions for photosynthesis productivity and dissolved oxygen generation.

SDT measurements are commonly used to infer lake turbidity. Turbidity is measured using several methods, but the easiest and least expensive method is through utilization of a secchi disk. All SDT measurements were collected on August 24, 2014, 1 day after the Landsat 8 image acquisition date. Calibration of remotely collected data requires site-based sampling that is nearly concurrent with remote data capture, illustrating that remote sensing is not entirely independent of field-based monitoring. (McCullough, Loftin, & Sader, 2012)

Regression equations have been commonly used to estimate water quality conditions from Landsat data (Brezonik, Menken, & Bauer, Landsat-based Remote Sensing of Lake Water Quality Characteristics, Including Chlorophyll and Colored Dissolved Organic Matter (CDOM), 2005). Regression equations are used to relate water quality characteristics, like SDT, to Landsat brightness values. For example, Powell et al. (2008) successfully used a regression equation to model the relationship between in-situ secchi disk transparency (SDT) data and lakes via landsat imagery using a linear regression model. Bonansea et al. (2015) also successfully used a regression equation to model the relationship of water quality parameters using Landsat TM and ETM + imagery. Both studies found success in relating SDT values to Landsat brightness values yet the two studies used different bands for their models. This tells us that the best band ratio may differ from one study to anther depending on band ratios and atmospheric interference (Brezonik, Menken, & Bauer, Landsat-based Remote Sensing of Lake Water Quality Characteristics, Including Chlorophyll and Colored Dissolved Organic Matter (CDOM), 2005).

Kloiber et al. (2002) tested many combinations of Landsat 5 bands and then narrowed down the band combinations to a ratio of bands 1 and 3 that were a reliable predictor of SDT. They found that when the regression models used r^2 values for brightness data, measured SDT decreased with increasing size of the time window between image collection and ground observation SDT. Kloiber's study examined all lakes within the state of Michigan. Their regression model, (In(SDT) = a(TM1/TM3) + bTM1 + c), was applied be applied to all lakes within the study area.

Study Area

Figure 2: Study Area

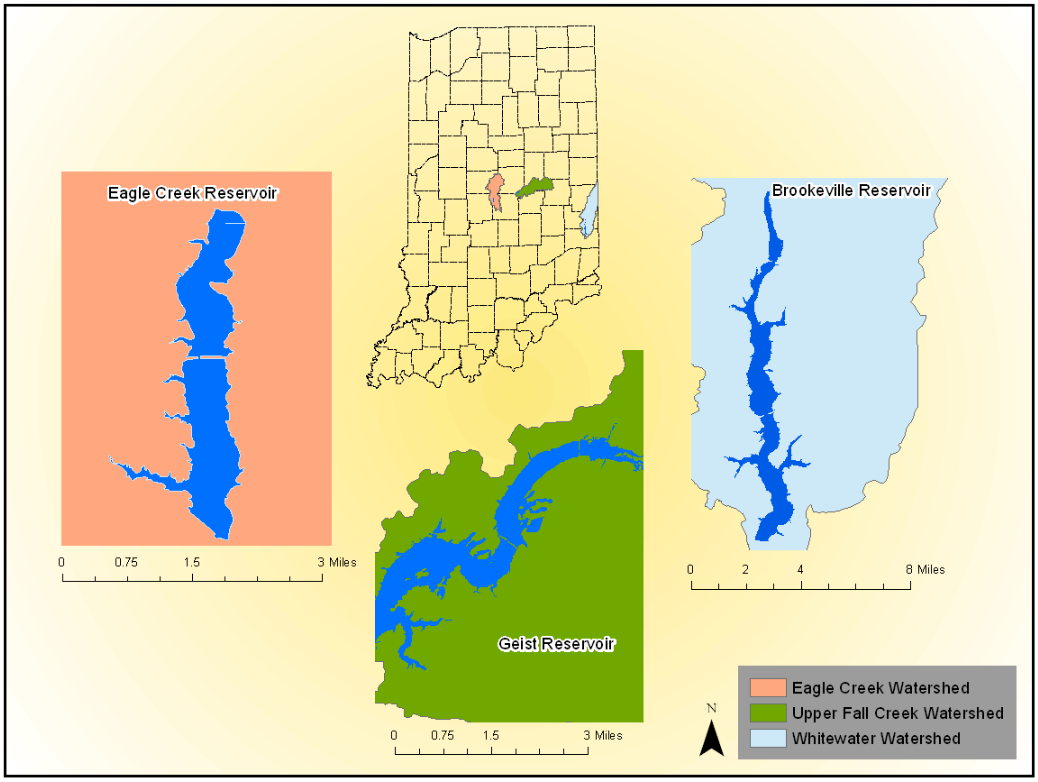

Brookville Reservoir

Brookville Reservoir is located in Southeastern Indiana and covers portions of Union and Franklin counties. It was constructed in 1974 by the United States Army Corps of Engineers for flood control, storm water management, and recreational activities. Communities in this area rely on Brookville Reservoir for their potable water supply as much of Southeastern Indiana does not have an adequate groundwater supply. It has a surface area of 8.2 square miles and a maximum capacity of 359,600 acre-feet. The maximum depth of the reservoir is 140 feet with an average depth of 30 feet. The Whitewater River and other tributaries feed the reservoir. The contributing watershed to the reservoir is 381.7 mi^2 (Indiana Department of Natural Resources, 2011).

Geist Reservoir

Geist Reservoir in central Indiana spans three counties: Marion, Hamilton, and Hancock. It was built in 1944 to provide a consistent source of potable water supply to the Citizen's Water Fall Creek drinking water treatment plant. Geist is characterized as a shallow turbid water body with an average depth of 11 feet. The reservoir has a maximum depth of 48 feet and a maximum storage capacity of 60,000 acre-feet. Its normal capacity is 21,175 acre-feet. The surface area of the reservoir is 2.96 mi^2 with a short hydraulic retention time of 58 days. The reservoir is fed by Fall Creek from the North. The contributing watershed to the reservoir is 218.95 mi^2 (V3 Companies, 2011).

Eagle Creek

Eagle Creek Reservoir is located in Marion County. Dam construction began in 1966 and was completed in 1969. The dam was built to control flooding on the Big Eagle Creek, a tributary of the White River. There is one potable water supply intake structure located on the Northeast side of the reservoir that supplies drinking water to customers of Citizens Water. The reservoir has a surface area of 2.16 mi^2 and a maximum pool elevation of 811.5 feet above sea level (Eagle Creek Advisory Committee, 1997).

Methods

Predicting SDT from a Landsat image first begins with collecting field data. Once the data is collected it is digitized and brought into an analysis program. For this study, the digitized data was brought into ERDAS Imagine. Next, satellite imagery from approximately the same date (within 1 day) as the field data was obtained from the USGS Global Visualization Viewer. The field data was then compared to the satellite data by creating areas of interest (AOI) inside the satellite image above the location of the field collected sample sites. A regression analysis was used to calibrate field data with the spectral data in the form of brightness values of the image. Trial regression equations were executed on various ban combinations because, as stated previously, the best band ratio differs from study to study depending on band ratio and atmospheric conditions (Brezonik, Menken, & Bauer, 2005). One regression analysis should be used for each image (Olmanson, Kloiber, Bauer, & Brezonik, 2001). As only one image was used for this study, only one regression analysis was necessary. Lastly, the regression analysis with the highest correlation was used to develop a model that was then be applied to Geist and Eagle Creek Reservoirs to satellite estimated SDT.

Field Data Collection

In situ measurements must be collected in order to develop a quantitative relationship among the field data and the landsat sensor data (Jensen J. R., 2007). SDT was measured at Brookville Reservoir using a standard 20 centimeter diameter secchi disk with alternating black and white quadrants. The secchi disk was then lowered into the water column until it could no longer be seen. The SDT or lake turbidity is then determined at the point in which the disk disappears from view (Fuller & Minnerick, 2001-2006). Careful planning and consideration is needed to collect SDT measurement as there are many factors that will affect the secchi disk reading. Some of those factors include, water color, wind, waves, sunlight, sample collector's eye sight (Indiana Clean Lakes Program, 2011). The best time to take a secchi disk reading is on a calm day when the sky is clear. The angle of the sun can cause interference seeing the secchi disk underwater so working between the hours of 10 a.m. to 4 p.m. is ideal. Secchi disk readings should also only be taken when surface winds are low so as to not create high waves. Waves on the water may create specular reflections which can cause problems as the satellite sensor collects radiance data from the area (Jensen J. R., 2007). Water transparency may be diminished after a strong rain event or during heavy boating activity (Indiana Clean Lakes Program, 2011).

Field samples must be taken from un-vegetated water in order to form empirical relationships between Landsat 8 and SDT (Olmanson, Kloiber, Bauer, & Brezonik, 2001). As it was important to take SDT samples from un-vegetated areas, sampling locations at the northern most point of Brookeville were not possible due to algal blooms proliferating at the time of sampling (Figure 3).

Figure 3: SDT Sample Locations

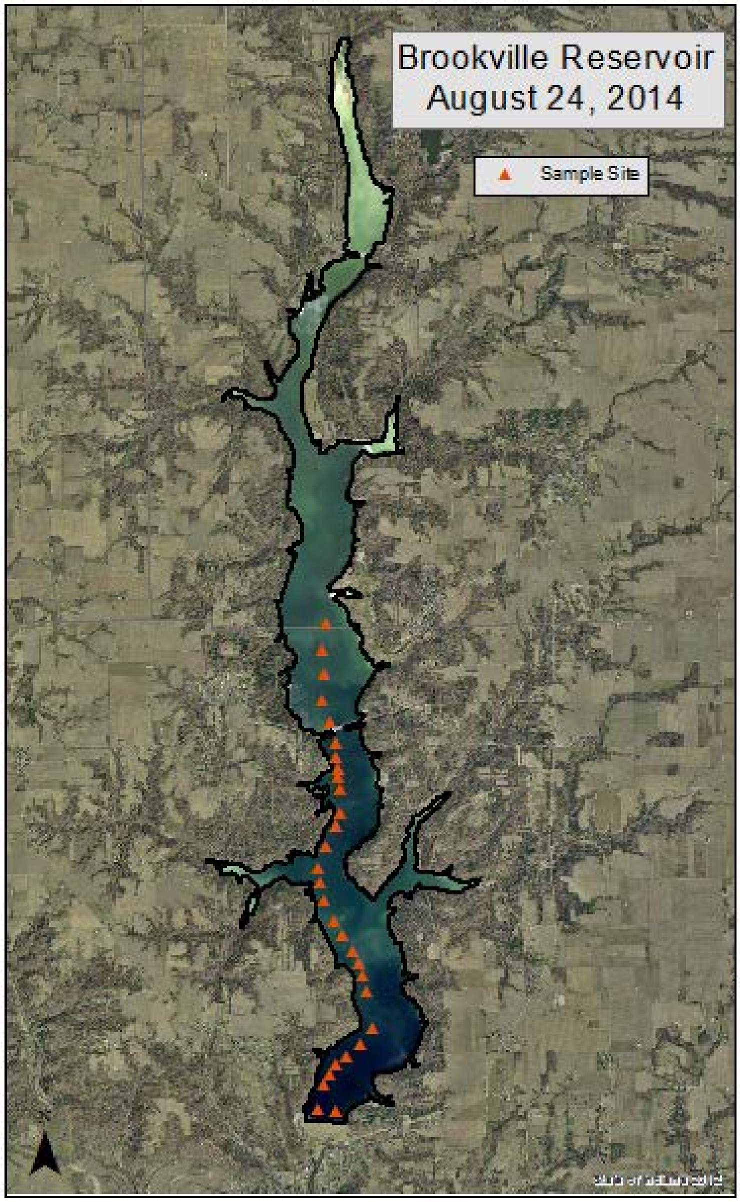

Sampling locations were limited to areas where the water was at least 15 feet deep so the reflectance from vegetation, shorelines, or lake bottom would not affect the spectral signature when processing the image per the advice of Olmanson et al. (2001). Prior to using the SDT string, using a tape measure, every inch was marked to allow for reading the depths with the SDT in the water. At each location, the “SDT Down” depth was obtained by lowering the disk into the water on the shady side of the boat until the disk was no longer visible. Next, the "SDT Up" depth was obtained by raising the disk until it became visible again. Both SDT depths were recorded at each location. Finally, the SDT depths at each location were then averaged to get the mean SDT depth (see Table 3 below).

Table 3: SDT Sample Locations and SDT Depths

Sample Location	Northing_Y	Easting_X	SDT(in) Down	SDT(in) Up	MeanSDT(in)
1	4,376,934.12	672,128.61	32.25	28.00	30.13
2	4,376,441.51	672,062.60	32.50	28.50	30.50
3	4,375,972.87	672,077.07	36.00	34.00	35.00
4	4,375,504.97	672,063.67	39.25	36.88	38.06
5	4,375,047.73	672,079.10	35.50	32.50	34.00
6	4,374,795.78	672,232.63	43.50	39.25	41.38
7	4,374,434.94	672,190.90	35.00	37.25	36.13
8	4,374,166.98	672,240.20	42.00	40.00	41.00
9	4,373,895.58	672,232.03	41.00	38.00	39.50
10	4,373,589.22	672,253.79	37.50	36.00	36.75
11	4,373,335.21	672,303.47	39.00	37.00	38.00
12	4,373,136.57	672,223.67	42.50	40.00	41.25
13	4,372,529.28	672,076.73	44.00	42.00	43.00
14	4,372,280.45	671,918.57	42.75	41.00	41.88
15	4,371,996.64	671,921.84	45.50	44.00	44.75
16	4,371,616.01	671,988.34	46.00	44.75	45.38
17	4,371,254.87	672,145.72	44.25	39.50	41.88
18	4,371,042.66	672,234.14	42.50	41.50	42.00
19	4,370,675.42	672,384.32	42.50	40.50	41.50
20	4,370,486.00	672,488.80	43.25	42.50	42.88
21	4,370,334.33	672,625.85	42.00	40.25	41.13
22	4,370,005.91	672,709.36	39.00	37.75	38.38
23	4,369,302.80	672,816.99	39.88	38.50	39.19
24	4,369,104.51	672,622.27	53.75	52.50	53.13
25	4,368,905.25	672,366.96	50.25	48.25	49.25
26	4,368,735.55	672,167.28	48.13	47.50	47.81
27	4,368,515.28	672,055.68	51.25	50.13	50.69
28	4,368,219.45	671,964.87	50.50	49.25	49.88
29	4,367,598.59	671,966.88	53.00	51.50	52.25
30	4,367,553.66	672,404.13	53.50	52.00	52.75

The number of sample sites was based on Olmanson et al.(2013), which determined that approximately 30 well-distributed ground control points was sufficient, resulting in a positional accuracy of + .25 pixels, or 7.5 meters. This was achieved using a Trimble ™ Geo 7 with an accuracy of .05 meters. The boat was maneuvered to each sampling location with the location being recorded by the Trimble GPS device.

In-situ data collection took place at Brookville Lake between the hours of 10:00 am and 3:00 pm on August 24, 2014. The original data collection date was August 8, 2014; however, that day was extremely cloudy due to storms in the area. August was chosen as the sample month due to typical short-term variability in lake water clarity and lakes having recordable water turbidity (Olmanson, Kloiber, Bauer, & Brezonik, 2001). Algal blooms reach maximum size in August or September as warm summer temperatures peak (Kudela, et al., 2015). From the 30 secchi disk samples that were collected, the range of the data was 23 inches and the standard deviation was 5.836509 inches.

Satellite Data

One Landsat 8 scene from the USGS Global Visualization Viewer for August 24th, 2014 was downloaded. The downloaded image is located on path 21 row 32 (see Figure 4 below).

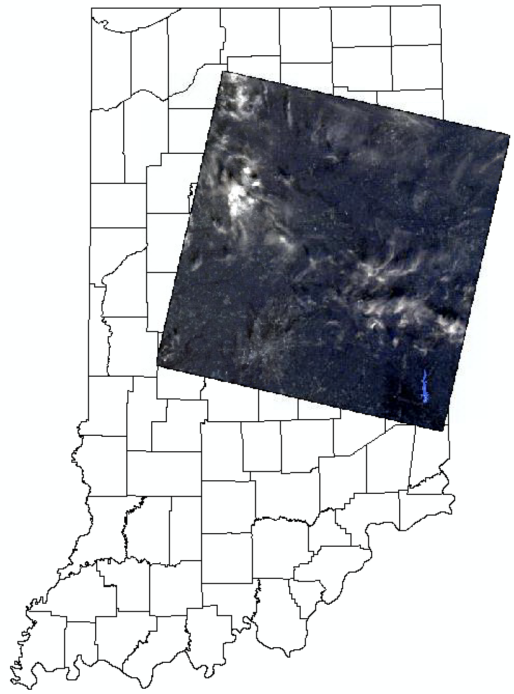

Figure 4: Landsat 8 Study Image

Natural Color composite downloaded scene of Path 21 Row 32 from Glovis.USGS.Gov displayed using bands 4,3,2 with overlay of Brookville Reservoir shapefile.

This study utilized calibrated Landsat 8 data with ground-based SDT measurements for Brookville Lake. The model developed for Brookville Lake was used to estimate SDT distributions in Eagle Creek and Geist Reservoirs. As Olmanson et al. (2001) mention, SDT depth should be reported as satellite-estimated SDT values rather than the general term of SDT. The reason for this is that there are other factors besides algal turbidity that play a part in lake clarity. A factor that influences the strength of the relationship between field-collected data and satellite data is the number of pixels included in the area of interest (AOI) (Kloiber, Brezonik, Olmanson, & Bauer, 2002).

In-situ data collection took place contemporaneously with satellite image acquisition; as a result, only a small cluster of pixels containing ground data will give the best correlations as determined by data analysis trials. It was determined that when the 30 samples locations or AOIs had a range of 7 pixels the R^2 value equaled 0.580246. When those same 30 AOIs had a range of 475 pixels the R^2 value equaled 0.456423, thus increasing the AOI yielded marginal benefits.

It is noted that the average brightness data from at least nine pixels in the deep open area of the lake should be used to predict lake clarity. Kloiber et al. (2002) also writes, increasing from nine pixels in the AOI did not increase the value and, as long as in-situ data collection were contemporaneous with the satellite image, a small group of AOIs would provide the best correlations between satellite and in-situ measurements. This, too, was the case for the Brookville area study. Increasing the pixel size reduced the accuracy of the model, as shown in Table 4.

Table 4: Pixel Size vs Accuracy

# of AOI	Pixel Range	R^2	Significance F
30	475	0.456423	0.000266703
30	7	0.580246	8.13644E-06

Utilizing Satellite Imagery to Estimate SDT

Water Only Image

To reduce image size, three water-only images of Brookville, Eagle Creek, and Geist reservoirs were created from the image downloaded from Glovis.USGS.Gov. The benefit of creating a water-only image is to conserve file space by removing unnecessary data and to create an unsupervised classification lake map to act as a guide for selection of the AOIs. The unsupervised classification images identify classes of pixels that are affected by varying algae concentrations. Ten different classes were used in the unsupervised classification step, and the classes were color-coded by variations in water quality. Classes that highlighted vegetation, shoreline, and bottom effects were avoided when choosing sample (AOI) locations on Geist and Eagle Creek Reservoirs. See unsupervised classification Geist map below.

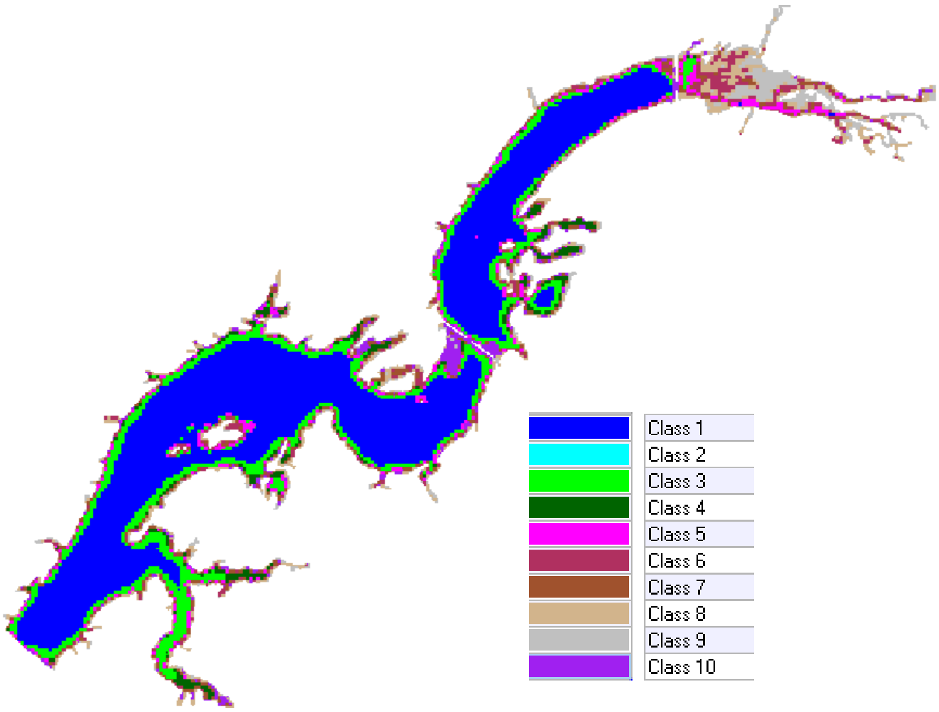

Figure 5: Unsupervised Classification map of Geist reservoir used as a guide to differentiate vegetation and other classes when selecting AOIs.

Area of Interest (AOI) Creation (Brookville Lake)

One shapefile of 30 sample locations was created corresponding to the collected SDT measurements at Brookville Lake. This shapefile was then opened on top of the Landsat satellite scene in Erdas IMAGINE. AOIs were digitized around the SDT measurements for the Brookville Lake water-only scene. The smallest AOI was 10 pixels and the largest AOI was 17. Once all the AOIs were drawn around the sample site locations within the satellite scene, each AOI was added to the signature file. The location ID, pixel count, mean band brightness value, measured SDT, and lnSDT for each band within the AOI was computed. These results were then exported into a .dat file format for further calculation. Results for the measurement values within the corresponding AOIs can be seen in TABLE 5 on next page.

Table 5: Brookville AOIs

SigName	PixelCount	Mean(Green Band)	Mean(Red Band)	Red Band:Green Band	meanSDT(m)	ln(sdt)m
Location 1	17	7058.17	6188.82	0.87	0.76	-0.26
Location 2	10	6995.90	6122.50	0.87	0.77	-0.25
Location 3	10	7022.20	6130.60	0.87	0.88	-0.11
Location 4	17	6955.17	6108.05	0.87	0.96	-0.03
Location 5	15	7109.66	6201.26	0.87	0.86	-0.14
Location 6	10	6905.70	6064.00	0.87	1.05	0.05
Location 7	10	6890.50	6070.80	0.88	0.91	-0.08
Location 8	12	6918.66	6071.58	0.87	1.04	0.04
Location 9	10	6911.30	6059.80	0.87	1.00	0.03
Location 10	10	6901.60	6073.90	0.88	0.93	-0.06
Location 11	10	6876.22	6048.11	0.88	0.96	-0.03
Location 12	10	6914.50	6051.70	0.87	1.04	0.04
Location 13	17	6928.47	6068.41	0.87	1.09	0.08
Location 14	14	6934.42	6068.00	0.87	1.06	0.06
Location 15	10	6945.10	6078.80	0.87	1.13	0.12
Location 16	13	7056.30	6139.92	0.87	1.15	0.14
Location 17	10	6992.30	6121.80	0.87	1.06	0.06
Location 18	16	6909.31	6056.87	0.87	1.06	0.06
Location 19	16	6916.93	6063.62	0.87	1.05	0.05
Location 20	17	6912.05	6052.00	0.87	1.08	0.08
Location 21	14	6901.28	6052.28	0.87	1.04	0.04
Location 22	12	6845.08	6029.00	0.88	0.97	-0.02
Location 23	12	6828.33	6012.91	0.88	0.99	-0.05
Location 24	14	6816.07	6015.42	0.88	1.35	0.30
Location 25	15	6823.20	6016.20	0.88	1.25	0.22
Location 26	16	6824.00	6015.18	0.88	1.21	0.19
Location 27	15	6796.06	5998.53	0.88	1.28	0.25
Location 28	14	6773.57	5993.50	0.88	1.26	0.23
Location 29	10	6799.70	5996.80	0.88	1.32	0.28
Location 30	10	6794.00	5992.00	0.88	1.34	0.29

Geist and Eagle Creek Reservoirs AOIs

After opening the water-only images of Geist and Eagle Creek (and using an unsupervised classification map as a guide), AOIs were selected for each of these reservoirs. For best results, these AOIs should be chosen from areas within the lakes that best represent it while avoiding areas affected by bottom, shoreline or vegetation effects (Olmanson, Kloiber, Bauer, & Brezonik, 2001). The location ID, pixel count, and mean band brightness value for each band within the AOI was computed. These results were then exported into a .dat file format for further calculation. As no in-situ measurements were recorded at these two reservoirs, the mean brightness value data was used in the final model to generate predicted SDT. An example of the AOI selection can be seen in FIGURE 6.

Figure 6: AOI Selection of Eagle Creek

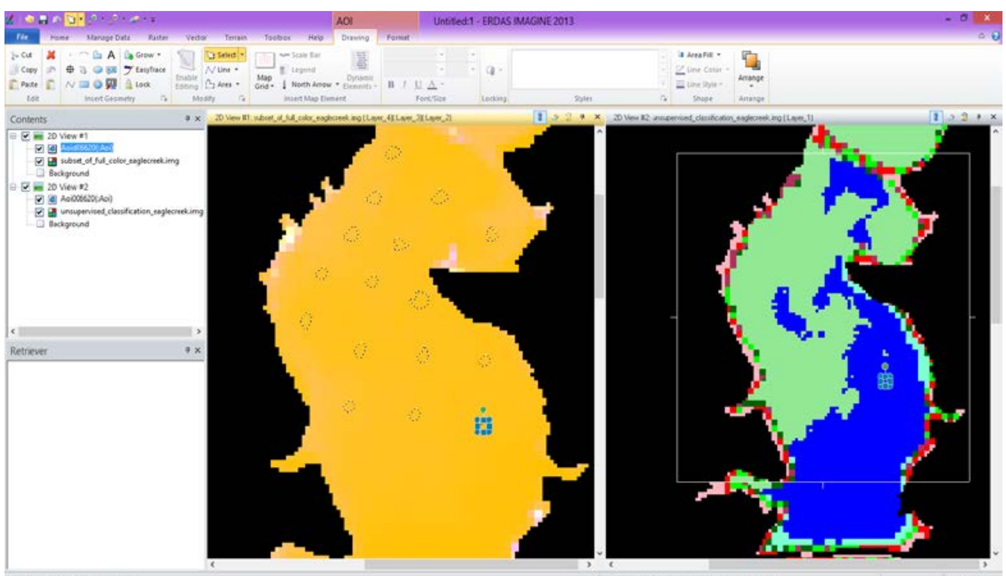

Results

Regression Equations and Tests of Significance

With brightness values obtained for 30 AOIs in Brookville reservoir, trial regression analysis were computed for Brookville Reservoir based on the equation developed by Kloiber et al. (2002):

$$\ln(SDT) = a(TM1/TM3) + bTM1 + c$$

As the Kloiber et al. equation addressed satellite imagery from Landsat 7, further regression analysis was needed to verify which Landsat 8 bands had the best correlation values. Analysis focused on Landsat 8 combinations of band 2, band 3, and band 4. As is noted in TABLE 6, band 4/band 3 + band 4 had the strongest relationship with SDT (R^2=.58, Significance F= 8.13644E-06).

Table 6: Band Combinations Trials

Blue Band : Red Band	
R^2	0.5590
Significance F	1.58E-05
Green Band: Red Band	
R^2	0.5783
Significance F	8.65E-06
Red Band: Green Band	
R^2	0.5802
Significance F	8.14E-06
Red Band: Blue Band	
R^2	0.5589
Significance F	1.59E-05
Blue Band: Green Band	
R^2	0.4901
Significance F	0.0001
Green Band: Blue Band	
R^2	0.4881
Significance F	0.0001

Therefore, the final model to convert satellite image brightness values to predicted ln(SDT) is:

ln(SDT)=a(Band4:Band3)+b(Band4)+c. The corresponding SDT predicted values can then be calculated by the following equation: e^(ln(SDT)) = SDT.

The data was transferred into Excel's Analysis ToolPak for multiple regression calculations. The regression equations and data are listed below in TABLE 7. A further breakdown of the final model is listed in TABLE 8.

The resultant r^2 value of this study (r^2=0.5802) was less than the r^2 value obtained in the Kloiber et al. study of r^2=0.67. Some differences between the numbers was expected as the band wavelengths for the two studies were different. It was hoped that the Landsat 8 r^2 values would be higher as the Landsat 8 band wavelengths are narrower than the bands used in the study be Kloiber et al. A table with the final predicted SDT values for Geist and Eagle Creek reservoirs is shown in Table 9.

Table 7: Regression Data

Regression Statistics	
R Square	*0.5802*
Significance F	*8.1364E-06*
	Coefficients
Intercept	24.9021
X Variable 1	-10.4643
X Variable 2	-0.0026

Table 8: Final Model

"Y = (X Variable 1)(MeanRedBand:MeanGreenBand) + (X Variable 2)(MeanRedBand) + Intercept "

"ln(SDT) = -10.4643(MeanRedBand:MeanGreenBand) - 0.0026(MeanRedBand) + 24.9021"

"SDT = EXP(ln(SDT))"

Table 9: Predicted vs. Actual SDT

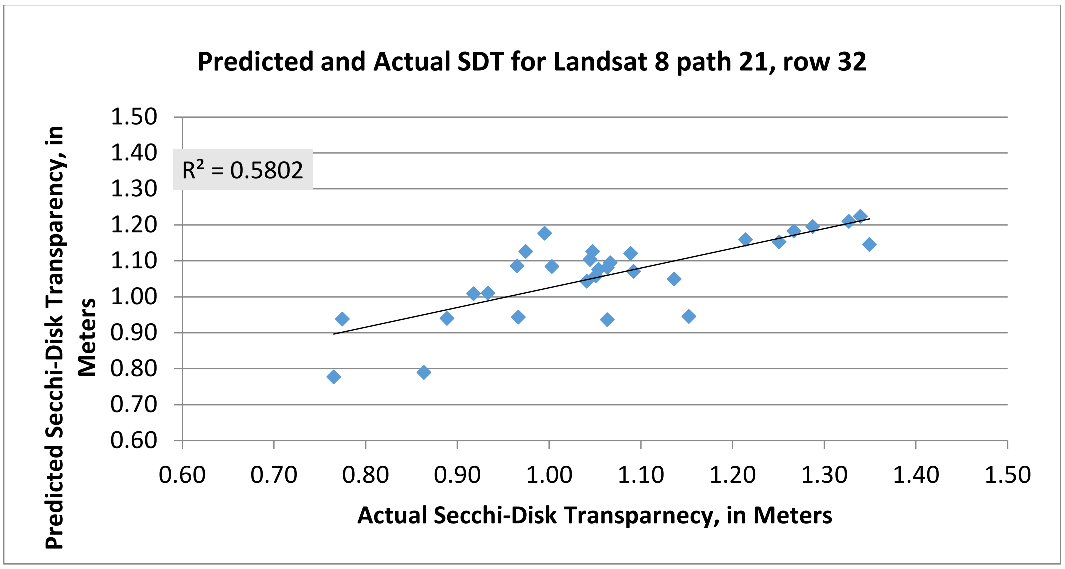

Table 10: Predicted SDT values for Eagle Creek and Geist Reservoirs.

Geist		Eagle Creek	
Location	SDT (m)	Location	SDT (m)
1	0.2283	1	0.4619
2	0.2329	2	0.4318
3	0.6136	3	0.4520
4	0.4852	4	0.3450
5	0.6595	5	0.3900
6	0.6283	6	0.2303
7	0.6573	7	0.2862
8	0.4882	8	0.3929
9	0.3268	9	0.3079
10	0.5085	10	0.4572
11	0.5027	11	0.3521
12	0.5434	12	0.3896
13	0.5146	13	0.4561
14	0.5985	14	0.4481
15	0.5623	15	0.4479
16	0.5598	16	0.4315
17	0.5244	17	0.4305
18	0.5442	18	0.3660
19	0.5499	19	0.4117
20	0.5787	20	0.4399
21	0.6352	21	0.4313
22	0.6239	22	0.4405
23	0.6181	23	0.5603
24	0.6025	24	0.5466
25	0.6462	25	0.5536
26	0.5883	26	0.5405
27	0.6430	27	0.5772
28	0.6575	28	0.5762
29	0.6889	29	0.5443
30	0.6840	30	0.5493
31	0.6821	31	0.5710
32	0.7099	32	0.5405
33	0.6888	33	0.5680
34	0.6659	34	0.5750
35	0.6818	35	0.5632
36	0.6348	36	0.5683
37	0.6653	37	0.6107
38	0.6138	38	0.5829
39	0.6605	39	0.5905
40	0.6534	40	0.6117
41	0.6520	41	0.6329
42	0.6078	42	0.5952
43	0.6787	43	0.5909
44	0.7116	44	0.5818
45	0.7032	45	0.6176

Figure 7: Predicted SDT Map for Eagle Creek Reservoir

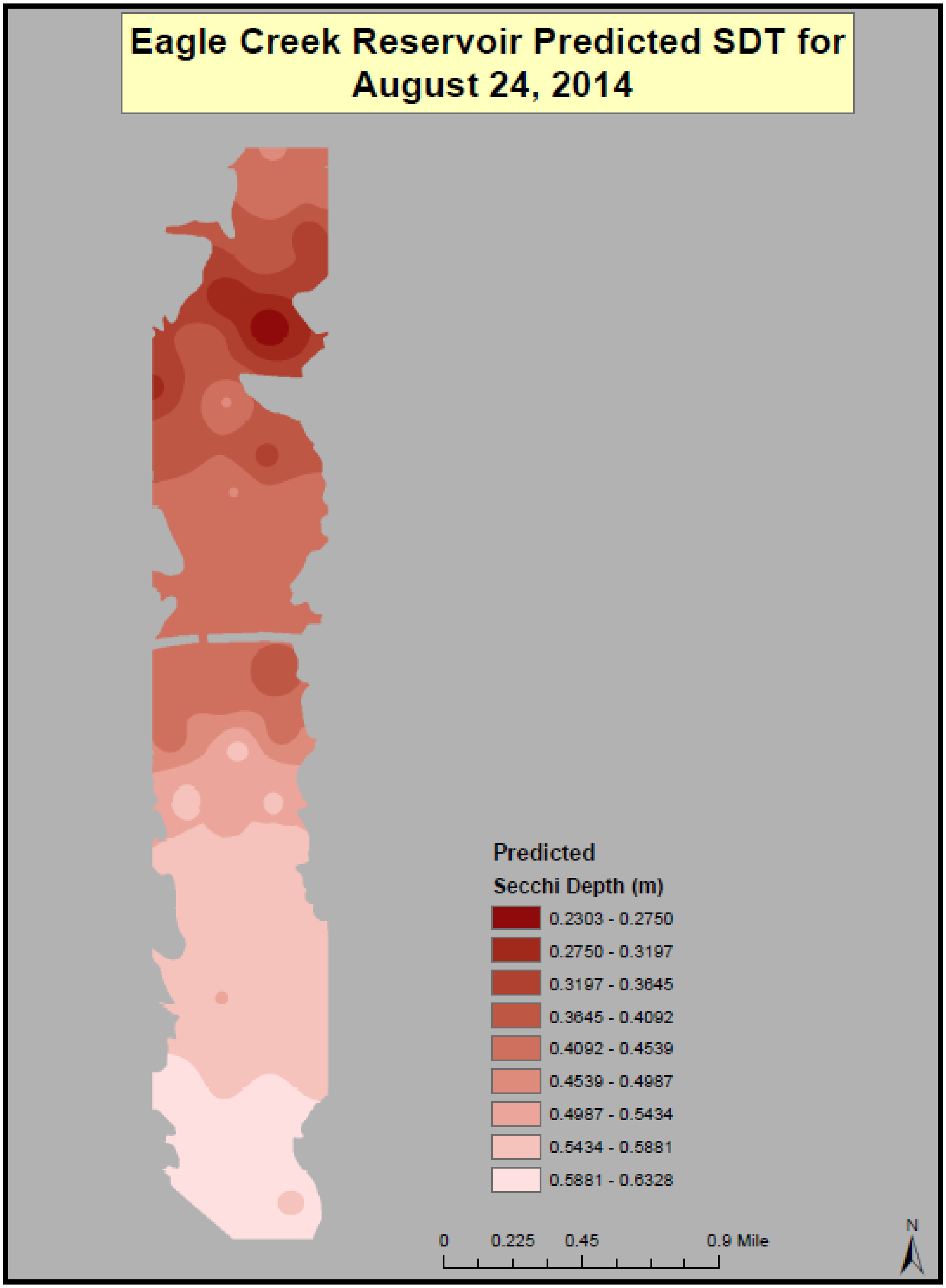

Figure 8: Predicted SDT Map for Geist Reservoir

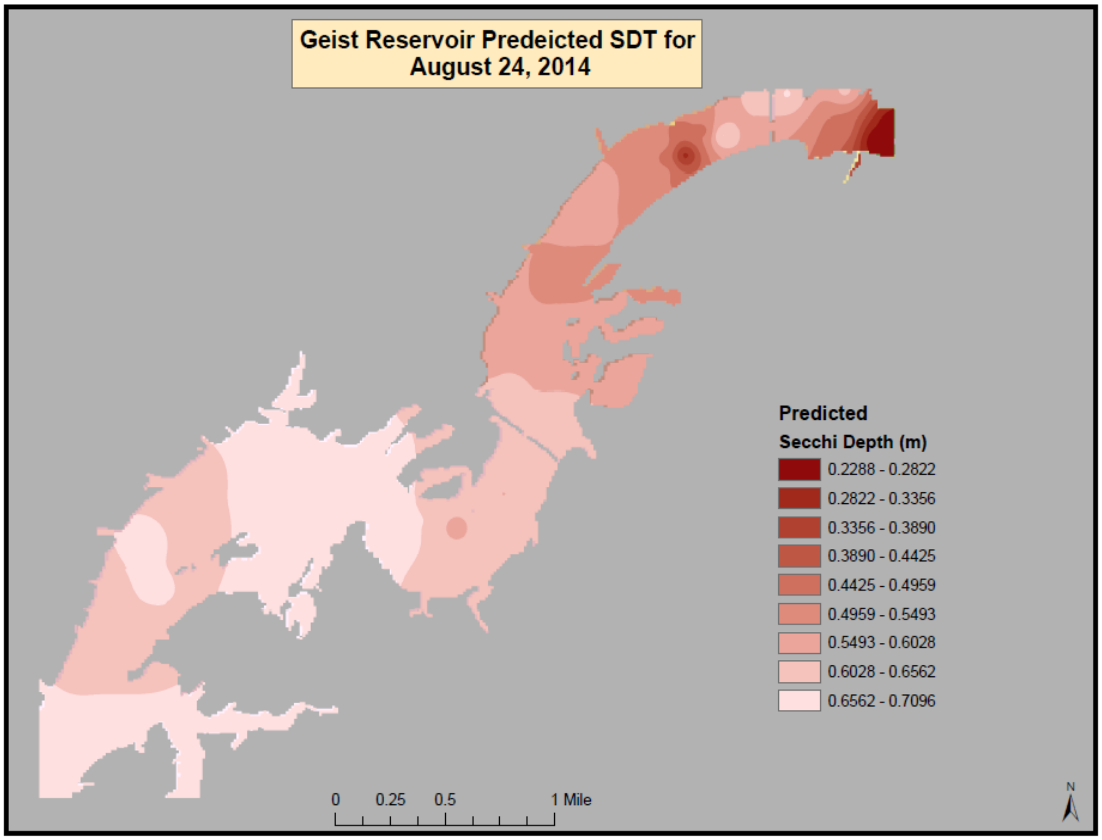

Conclusions

This study utilized a Landsat 8 satellite scene located in central Indiana and 30 SDT measurements to find the best method of predicting SDT for lakes in the same image. SDT data was collected at Brookville Reservoir on August 24, 2014. A regression model was developed to predict SDT levels at the unsampled reservoirs, Geist and Eagle Creek. The corresponding satellite image was downloaded to obtain the necessary brightness values. Regression analysis was performed using several different bands within Landsat 8. After comparing the calculated R2 and Significant F values for each of the different bands, a reasonable model was developed that can be used to predict SDT levels from the corresponding Landsat 8 images. SDT and turbidity have been shown to be highly correlated and act as a measure of algal abundance in Geist, Eagle Creek, and Brookville reservoirs. Red Band/Green Band + Red Band yielded the highest R2 and Significant F values and were used for further analysis on the un-sampled Geist and Eagle Creek Reservoirs to determine SDT depths. The results show that SDT can be estimated from Landsat 8 data as long as near contemporaneous in situ measurements are collected. These results confirm previous studies like Olmansen et al. (2002), Brezonik et al. (2005), Bonansea et al. (2015). These remote sensing techniques offer a low-cost method of water quality determination. Validation is necessary for the predictive model used to estimate SDT depth in the unsampled reservoirs. The secchi disk depth given for Geist and Eagle Creek are quantitative estimates and must be verified in order for this model to be useful.

Predictive models make assumptions related to distribution. In order to verify the predicted depths, residuals may be studied to further evaluate the validity of the model or in situ samples of the unsampled reservoirs will aid in the verification of predicted SDT depths.

Suggestions for future tests regarding water quality monitoring using secchi disk consist of taking samples before and after the image acquisition. This may be beneficial in establishing a more representative outline of SDT levels and help eliminate any doubt of secchi disk user calculation error that may have occurred due to the angle of the sun or varying conditions of the waterbody. With a more comprehensive dataset, a model could potentially be developed with a higher degree of correlation.

References

Bonansea, M., Rodriguez, M., Pinotti, L., & Ferrero, S. (2014). Using multi-temporal Landsat imagery and linear mixed models for assessing water quality parameters in Rio Tercero reservoir. *Remote Sensing of Environment*, 28-41.

Brezonik, P., Menken, K. D., & Bauer, M. (2005). Landsat-based Remote Sensing of Lake Water Quality Characteristics, Including Chlorophyll and Colored Dissolved Organic Matter (CDOM). *Lake and Reservoir Management*, 373-382.

Center for Earth and Environmental Science. (2015, March 3). *What causes algal blooms?* Retrieved from www.cees.iupui.edu/research: http://www.cees.iupui.edu/research/algal-toxicology/bloomfactors

Eagle Creek Advisory Committee. (1997). *Eagle Creek Park Master Plan.*

Fuller, L. M., & Minnerick, R. J. (2001-2006). *Predicting Water Quality by Relating Secchi-Disk Transparency and Chlorophyll-a Measurements to Landsat Satellite Imagery for Michigan Inland Lakes.* United States Geological Survey.

Indiana Clean Lakes Program. (2011). *Volunteer Lake Monitoring Manual.* Bloomington: School of Public and Environmental Affairs-Indiana University.

Indiana Department of Environmental Management . (2015, March 5). *Addressing Concerns About Blue-Green Algae* . Retrieved from http://www.in.gov/idem/algae/2310.htm#

Indiana Department of Natural Resources. (2011). *Brookville Reservoir Whitewater Memorial State Park Interpretive Master Plan.* Indiana Department of Natural Resources.

Jensen, J. R. (1983). Biophysical Remote Sensing. *Annals of the Association of American Geographers*, 111-132.

Jensen, J. R. (2007). *Remote Sensing of the Environment.* Upper Saddle River: Pearson Prentice Hall.

Kloiber, S. M., Brezonik, P. L., Olmanson, L. G., & Bauer, M. E. (2002). A procedure for regional lake water clarity assessment using Landsat multispectral data. *Remote Sensing of Environment*, 38-47.

Knight, J. F., & Voth, M. L. (2012). Application of MODIS Imagery for Intra-Annual Water Clarity Assessment of Minnesota Lakes. *Remote Sensing*, 2181-2198.

Kudela, R. M., Palacios, S. L., Austerberry, D. C., Accorsi, E. K., Fuild, L. S., & Torres-Peres, J. (2015). Application of hyperspectral remote sensing to cyanobacterial blooms in inland waters. *Remote Sensing of Environment*.

Landsat Science. (2014, June 6). Retrieved June 9, 2014, from NASA.GOV: http://landsat.gsfc.nasa.gov/?page_id=7195

McCullough, I. M., Loftin, C. S., & Sader, S. A. (2012). Combining lake and watershed characteristics with Landsat TM data for remote estimation of regional lake clarity. *Remote Sensing of Environment*, 109-115.

Olmanson, L. G., Kloiber, S. M., Bauer, M. E., & Brezonik, P. L. (2001). *Image processing protocol for regional assessments of lake water quality.* St. Paul: Water Reources Center and Remote Sensing Laborator University of Minnesota.

Powell, R., Brooks, C., French, N., & Shuchman, R. (2009). *Remote Sensing of Lake Clarity.* Ann Arbor: Michigan Tech Research Institute.

Roy, D. P., Wulder, M. A., Loveland, T. R., Woodcock, C. E., Allen, R. G., Anderson, M. C., . . . Zhu, Z. (2014). Landsat-8: Science and product vvision for terrestrial global change research. *Remote Sensing of Environment*, 154-172.

Schlacher, T. A., Lloyd, S., & Wiegand, A. (2010). Use of local ecological knowledge in the management of algal blooms. *Environmental Conservation* , 210-221.

Srriwongsitanon, N., Surakit, K., & Thianpopirug, S. (2011). Influence of atmospheric correction and number of sampling points on the accuracy of water clarity assessment using remote sensing application. *Journal of Hydrology*, 203-220.

Tebbs, E. J., Remediios, J. J., & Harper, D. M. (2013). Remote sensing of chlorophyll-a as a measure of cyanobacterial biomass in Lake Borgoria, a hypertrophic, saline-alkaline, flamingo lake using Landsat ETM+. *Remote Sensing of Environment*, 92-106.

U.S. Geological Survery. (2015, March 3). *Bands Designations for Landsat satellites* . Retrieved from Landsat.USGS.Gov: http://landsat.usgs.gov/band_designations_landsat_satellites.php

United States Environmental Protection Agency. (2013, February 15). *Impacts of Climate Change*. Retrieved from http://www2.epa.gov/sites/production/files/documents/climatehabs.pdf

V3 Companies. (2011). *Geist Reservoir/Upper Fall Creek Watershed Management Plan.*

Wynne, T. (2013, March 23). *NOAA Ocean Science Blog*. Retrieved from https://noaaoceanscience.wordpress.com/2013/05/23/nccos-continues-issuing-weekly-lake-erie-harmful-algal-bloom-forecasts/

CURRICULUM VITAE

Miranda J. Hancock

Education

Indiana University – Purdue University Indianapolis
M.S., Geographic Information Science
August 2015

Indiana University – Purdue University Indianapolis
B.A. Geography
May 2010

Professional Experience

Indiana Department of Environmental Management -- Indianapolis, IN --
August 2014-Present
Senior Environmental Manager

- Business process research and analysis
- Project management documentation outlining work structure, project schedule
- Conduct User Assistance Testing with Management, Permit Writers, and Administrative staff (SharePoint, Syncplicity, Modelers Utility)
- Develop user guides for Permit Writers, Administrative staff, and Management
- Conduct user trainings and continue post-implementation support for SharePoint and Modelers Utility (ArcMap)
- Stream Modeling/Wasteload Allocation analyses
- Provide cross functional networking with permittees, consultants, IDEM associates, and EPA to assure state regulatory compliance
- Develop statewide Industrial NPDES permits
- Conduct site visits with facilities, consultants, stakeholders
- Create and maintain geodatabases

Indiana Department of Environmental Management -- Indianapolis, IN --
August 2011-August 2014
Environmental Manager

- Developed statewide Industrial NPDES permits
- Provide cross functional networking with permittees, consultants, IDEM associates, and EPA to assure state regulatory compliance
- Developed CSO (combined sewer overflow) ArcMap utility
- Developed a paperless permitting system for entire permit branch utilizing SharePoint and ArcMap

- Draft Preliminary Effluent Limitations and possess wasteload allocation knowledge

The Polis Center at IUPUI – Indianapolis, IN—
June 2010 – August 2011
GIS Analyst

- Design, development, testing, implementation, and analysis of GIS applications and models
- Developed multi-hazard mitigation plans using ArcGIS for municipalities in Indiana
- Project management documentation outlining work structure, project schedule, timeline
- Seamline editing using advanced orthorectification software
- Orthoimagery QC
- Create and Maintain geodatabases
- Develop training curriculum for HAZUS-MH and ESRI users
- Map Modernization
- Graphic editing of feature datasets using latest versions of ESRI software

Indiana Department of Natural Resources – Indianapolis, IN—
September 2008 – June 2010
Engineering Assistant

- Collected, analyzed, and interpreted hydrologic information collect in field studies and assisted in displaying the information collected through ArcGIS
- Installed, maintained, serviced, and troubleshot sensing, recording, and communication equipment and instrumentation
- Review well logs containing statistical and technically hydrologic data collected in field

Indiana Department of Environmental Management – Indianapolis, IN --
Summer 2008
Ground Water Section, Intern

- Collected, analyzed, and interpreted hydrologic information collect in field studies and assisted in displaying the information collected through ArcGis
- Performed field water-quality measurements such as water temperature, specific conductance, pH, dissolved oxygen, and alkalinity
- Collected, processed, prepared, and delivered samples to lab for analyses
- Assembled, evaluated and prepared field and laboratory data for tabulation, analysis, and publication
- Installed, maintained, serviced, and troubleshot sensing, recording, and communication equipment and instrumentation
- Calibrated meters and analytical equipment using appropriate techniques and protocols